engineering proceedings

MDPI

Proceeding Paper

Effect of Violet Laser Irradiation on the Optical Properties of Polyvinyl Alcohol/Methyl Orange Composite Thick Films: A Model for Medical Applications †

Sarah Maysam Tareq [1], Nihal A. AbdulWahhab [1] and Addnan H. Al-araji [2,*]

[1] Department of Physics, College of Science, University of Babylon, Babylon 5001, Iraq; sarah.ali.scihigh223@student.uobabylon.edu.iq (S.M.T.); sci.nihal.abdllah@uobabylon.edu.iq (N.A.A.)
[2] Department of Medical Physics, Hilla University College, Babylon 5001, Iraq
* Correspondence: adnanhilla@hilla-unc.edu.iq
† Presented at the International Conference on Recent Advances in Science and Engineering, Dubai, United Arab Emirates, 4–5 October 2023.

Abstract: This study investigates the impact of violet laser irradiation on the optical properties of thick films composed of polyvinyl alcohol (PVA), methyl orange (MO), and their composite (PVA/MO). Aimed at exploring potential medical applications, the films were synthesized through a casting process involving the dissolution of PVA and MO in distilled water. The optical properties, including absorbance spectra, energy gaps, and various optical constants, were meticulously measured before and after exposure to laser irradiation. The results revealed a notable decrease in the absorbance spectra and optical constants, along with an increase in the energy gaps, suggesting a structural modification induced by the laser treatment. These findings hold significance for the advancement of materials with customized optical features, potentially serving as a model for future developments in optoelectronic and photovoltaic devices. The research outcomes provide a foundation for the exploration of polymers and dyes in medical applications, particularly in the realms of non-invasive surgical procedures and simulations.

Keywords: polyvinyl alcohol; methyl orange; laser irradiation; optical properties; photovoltaic applications; medical applications

Citation: Tareq, S.M.; AbdulWahhab, N.A.; Al-araji, A.H. Effect of Violet Laser Irradiation on the Optical Properties of Polyvinyl Alcohol/Methyl Orange Composite Thick Films: A Model for Medical Applications. *Eng. Proc.* **2023**, *59*, 236. https://doi.org/10.3390/engproc2023059236

Academic Editors: Nithesh Naik, Rajiv Selvam, Pavan Hiremath, Suhas Kowshik CS and Ritesh Ramakrishna Bhat

Published: 27 February 2024

1. Introduction

Polymers, derived from the Greek words "poly", meaning "many", and "mere", indicating "parts", refer to high-molecular-mass molecules that consist of numerous repeating structural units [1]. Polyvinyl alcohol (PVA), a synthetic polymer, gained widespread use in the early twentieth century and has become a pivotal water-soluble plastic. Its inherent versatility allows it to easily blend with various substances, rendering it ideal for diverse applications. PVA has been employed across multiple sectors—industrial, commercial, medical, and food—for the production of lacquers, resins, surgical threads, and food packaging materials that are in direct contact with food [2]. The potential of PVA to undergo crosslinking through chemical or physical means, amalgamate with different polymers or copolymers, and graft or copolymerize with various monomers facilitates the creation of intelligent hydrogels. These hydrogels are notable for their stimuli-responsive properties, which can be fine-tuned. Moreover, PVA hydrogels exhibit excellent compatibility with skin, tissues, mucosa, and blood [3]. The utility of PVA extends to the simulation of soft tissue deformation, which can significantly enhance the effectiveness and precision of therapeutic interventions and minimally invasive surgical procedures. For these simulations, tissue-mimicking phantoms that emulate the mechanical properties of human or animal tissues are indispensable [4]. The structural formula of PVA is depicted in Figure 1 [5].

Dyes are characterized as organic compounds designed to color substrates through absorption, adsorption, reaction, or deposition with a certain level of permanence [6]. Methyl orange, an organic dye with the chemical formula $(CH_2CH[CH_2CH(CH_3)_2])_n$, is one such compound [7,8]. This dye is represented in Figure 2 below [9].

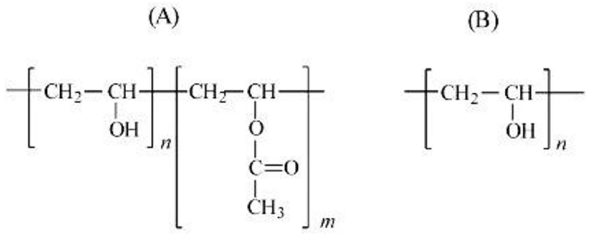

Figure 1. Structural formula of PVA: (**A**) Partly hydrolyzed; (**B**) Completely hydrolyzed.

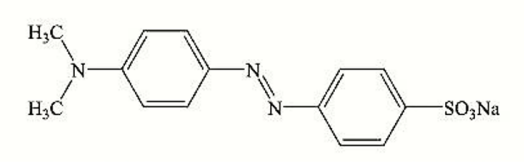

Figure 2. Structure of methyl orange dye.

A composite material is defined as an assembly composed of two or more distinct substances, where the resulting properties are superior to those of the individual constituents [10–13]. These materials have been integral in addressing engineering challenges and are now widely utilized in various applications, including the automotive industry [14–17]. When laser radiation encounters a surface, it undergoes reflection, absorption, and transmission. The Beer–Lambert law quantitatively describes the absorption process as light traversing a medium [18]:

$$I = I_0 e^{-\alpha t} \tag{1}$$

where I_0 and I denote the intensities of the incident and transmitted light, respectively, and α represents the absorption coefficient. The interaction between light and matter reveals the material's optical properties. When the photon energy $h\nu$ is equal to or surpasses the band gap energy E_g, it can excite a valence electron to the conduction band, generating an electron–hole pair. The threshold wavelength λ_c for this interaction is given by [19]:

$$\lambda(\text{nm}) = \frac{hc}{E_g} = \frac{1240}{E_g(\text{eV})} \tag{2}$$

Direct photon transitions within the material are governed by [20]:

$$\alpha h\nu = B(h\nu - E_g)^{\frac{1}{2}} \tag{3}$$

The optical characteristics of materials are those discovered when electromagnetic light strikes them [21]. The equation for reflectance, encompassing the sum of reflectance R, transmittance T, and absorbance A, is stated as [22]:

$$R + T + A = 1 \tag{4}$$

The absorbance A is determined through [22]:

$$A = \log\left(\frac{I_0}{I}\right) \tag{5}$$

This leads to the absorption coefficient α, calculated from the absorbance spectrum using [23]:

$$\alpha = \frac{2.303A}{t} \tag{6}$$

The extinction coefficient k is related to the absorption coefficient and the light's wavelength by [24]:

$$k = \frac{\alpha\lambda}{4\pi} \tag{7}$$

The refractive index n, representing the ratio of light's velocity in a vacuum to that within the material, can be calculated as [25]:

$$n = \sqrt{\left(\frac{4R}{(1-R)^2} - k^2\right)} + \frac{(1+R)}{(1-R)} \tag{8}$$

The real and imaginary parts of the dielectric constants of thick films are determined by [26]:

$$\epsilon_r = n^2 - k^2 \tag{9}$$

$$\epsilon_i = 2nk \tag{10}$$

The optical conductivity σ_{op} is influenced by the refractive index, speed of light, and absorption coefficient, as follows [19]:

$$\sigma_{op} = \frac{\alpha nc}{4\pi} \tag{11}$$

XRD is an invaluable non-destructive technique for characterizing materials, capable of discerning crystal structures, orientations, and sizes. The crystallographic planes are determined by Bragg's law [27]:

$$2d \sin\theta = n\lambda \tag{12}$$

2. Materials and Methods

Polyvinyl alcohol (PVA) and methyl orange (MO) powders, procured from Sigma-Aldrich Company (St. Louis, MI, USA), served as the primary materials in this study. A mass of 8 mg of PVA, with a molecular weight of 10,000 g/mol, and 7.5 mg of MO, with a molecular weight of 327.33 g/mol, were accurately weighed and dissolved in 7 mL of distilled water. The dissolution process was facilitated by heating the solution to 90 °C and maintaining continuous agitation with a magnetic stirrer for 10 min at room temperature, ensuring the complete solubility of both PVA and MO. Thereafter, the homogeneous solutions were cast into Petri dishes using the casting method and left to dry under ambient conditions, resulting in films with a nominal thickness of 3000 nm for each component, determined through a standardized gravimetric thickness measurement technique. The same protocol was employed to fabricate composite films of (PVA/MO), achieving a combined thickness of approximately 6000 nm under identical conditions. The films underwent irradiation by a 405 nm violet laser with an 80 mW power output for varying exposure times—10, 20, 30, and 40 min. The laser irradiation setup was calibrated to maintain a fixed distance between the laser source and the film surface, coupled with a heat sink to mitigate any thermal effects.

Post-irradiation, the optical properties of the films were quantified using a UV–Vis spectrophotometer (Model UV-1800 OA, Shimadzu, Kyoto, Japan) , with a spectral range of 190–1200 nm. To ascertain the transmittance and absorbance, the films were analyzed using the same instrument settings both before and after laser exposure. Fourier transform infrared (FTIR) spectroscopy was also conducted to characterize the PVA powder. The FTIR spectrum was acquired using an IR Affinity-1 spectrometer (Shimadzu Company,

Japan) with a detection range of 400–4000 cm^{-1}. Data analysis, including the calculation of the optical properties, was executed with specially tailored Excel-based software, ensuring rigorous adherence to established analytical methods in spectrophotometry.

3. Results and Discussion

The Fourier transform infrared (FTIR) spectroscopy analysis of the PVA powder is depicted in Figure 3. Notable peaks were observed in the spectrum, corresponding to various functional groups. The peak at 1263.42 cm^{-1} can be attributed to the carbonyl (-C-O) wagged vibration, whereas the peaks at 1375.29 cm^{-1} and 1570.11 cm^{-1} can be ascribed to the (C-H) and (CH2) wagged vibrations, respectively. Furthermore, the presence of the carbonyl (-C=O-) group was confirmed by a peak at 1722.49 cm^{-1}, which is indicative of the occurrence of a PVA reaction [28].

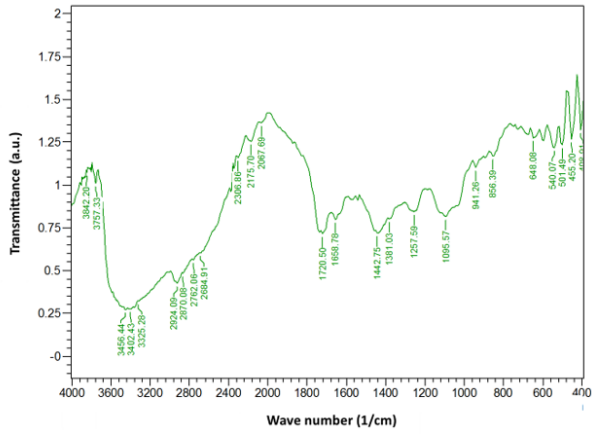

Figure 3. FTIR spectrum for PVA powder.

Figure 4 presents the FTIR spectrum for the MO powder. The strong peak detected at approximately 1280 cm^{-1} can be attributed to the C-S bond of the sulfonate group. Additionally, a weak band near 3300 cm^{-1} suggests the presence of an amine group. The significant peaks at around 1350 cm^{-1} are indicative of the C-N stretch of aromatic amine, which confirms the presence of the aromatic amine within the compound. The peak at around 1290 cm^{-1} denotes the S-O bond [29].

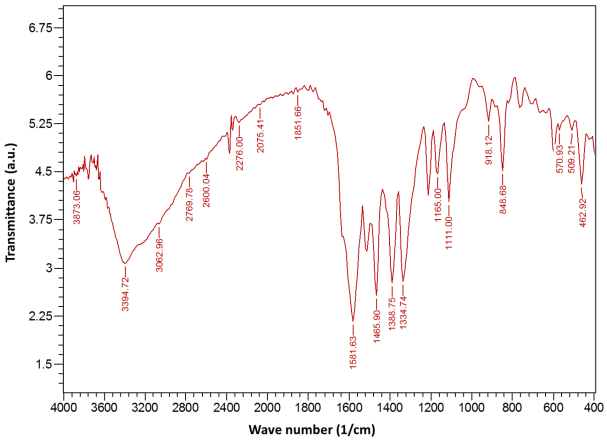

Figure 4. FTIR spectrum for MO powder.

The X-ray diffraction (XRD) patterns for pure PVA are exhibited in Figure 5. The XRD pattern reveals a distinct diffraction band at $2\theta = 19.4°$, characteristic of the semicrystalline nature of PVA. This semicrystallinity is likely due to the extensive intra-molecular hydrogen bonding within the PVA monomer units, as well as the inter-molecular hydrogen bonds among different monomer units [30]. The UV–Visible absorption spectra for the PVA, MO,

and PVA/MO thick films, both before and after laser irradiation at varying times (0, 10, 20, 30, and 40 min), were examined.

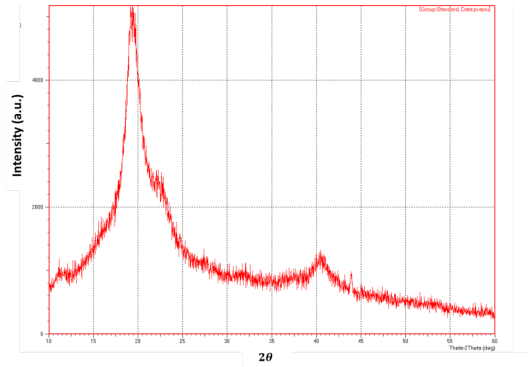

Figure 5. XRD pattern for PVA powder.

PVA exhibited an absorption peak at 350 nm, MO at 471 nm, and the PVA/MO composite at around 480 nm, with no significant absorption peaks at longer wavelengths. With increasing irradiation times, a decrease in absorption was observed across all film thicknesses. This trend is depicted in Figures 6a, 7a, and 8a, while the absorption spectra as a function of irradiation time are shown in Figures 6b, 7b, and 8b.

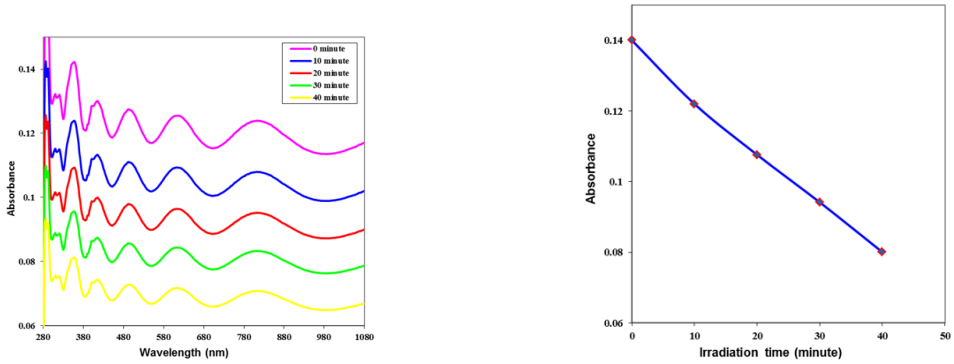

(**a**) (**b**)

Figure 6. PVA absorbance spectra and absorbance as a function of irradiation time: (**a**) Absorbance spectra of PVA for different laser exposure times (0, 10, 20, 30, and 40 min); (**b**) Absorbance as a function of irradiation time for PVA at a 350 nm wavelength.

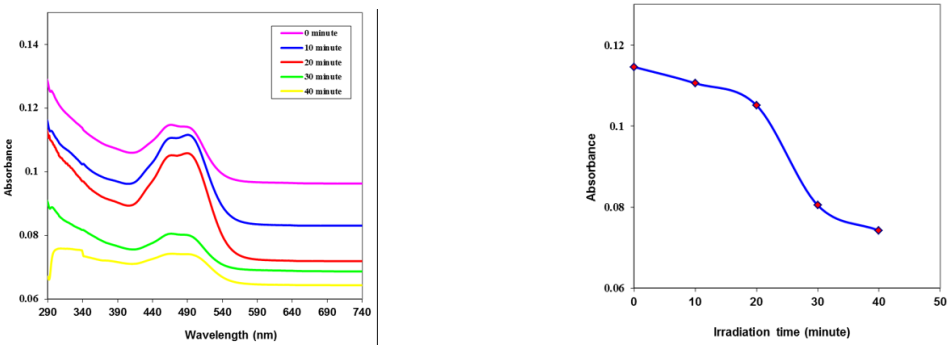

(**a**) (**b**)

Figure 7. MO absorbance spectra and absorbance as a function of irradiation time: (**a**) Absorbance spectra of MO for different laser exposure times (0, 10, 20, 30, and 40 min); (**b**) Absorbance as a function of irradiation time for MO at a 471 nm wavelength.

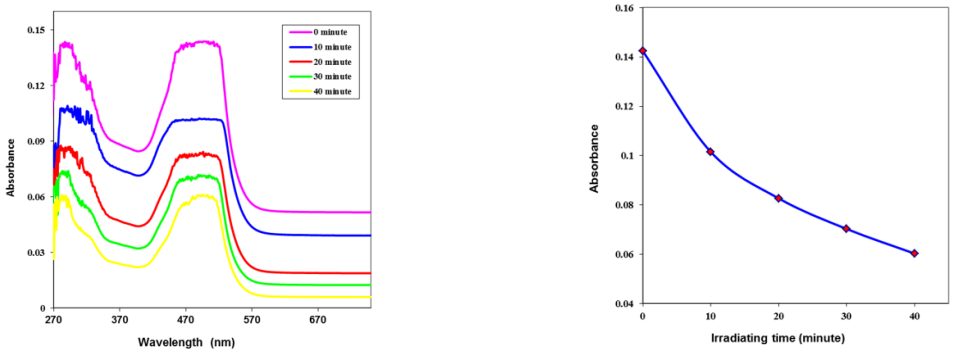

(**a**) (**b**)

Figure 8. PVA/MO absorbance spectra and absorbance as a function of irradiation time: (**a**) Absorbance spectra of PVA/MO for different laser exposure times (0, 10, 20, 30, and 40 min); (**b**) Absorbance as a function of irradiation time for PVA/MO at a 480 nm wavelength.

Figures 9–11 illustrate the energy gap calculations using Tauc's method for PVA, MO, and PVA/MO, respectively. The squared product of the absorption coefficient and photon energy ($(\alpha hv)^2$) was plotted against the photon energy for various irradiation times. An increase in the violet laser irradiation time led to a corresponding increase in the direct energy gap, as evidenced in Figures 9b, 10b, and 11b. This phenomenon, marked by a decrease in the absorption coefficient, is a pivotal feature for photovoltaic applications.

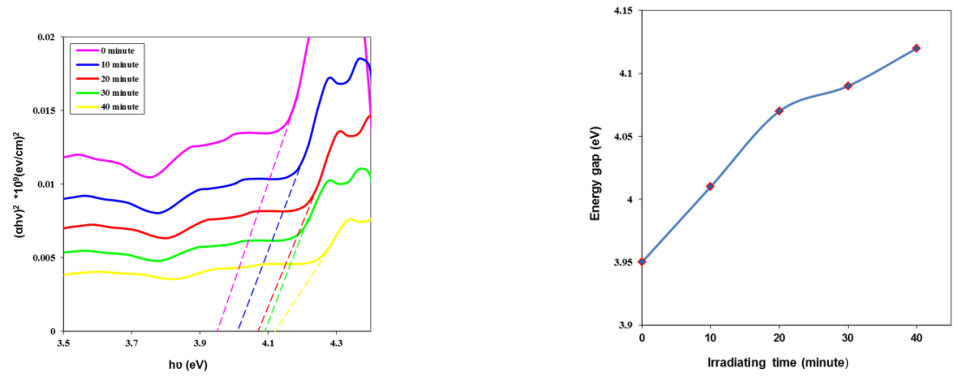

(**a**) (**b**)

Figure 9. PVA energy gap and direct energy gap as a function of irradiation time: (**a**) Energy gap $(\alpha hv)^2$ for PVA at different laser irradiation times (0, 10, 20, 30, and 40 min); (**b**) Direct energy gap as a function of irradiation time for PVA at a 350 nm wavelength.

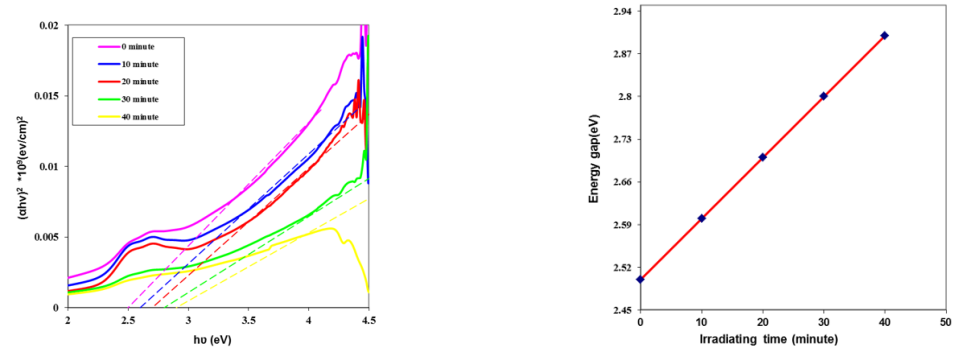

(**a**) (**b**)

Figure 10. MO energy gap and direct energy gap as a function of irradiation time: (**a**) Energy gap $(\alpha hv)^2$ for MO at different laser irradiation times (0, 10, 20, 30, and 40 min); (**b**) Direct energy gap as a function of irradiation time for MO at a 471 nm wavelength.

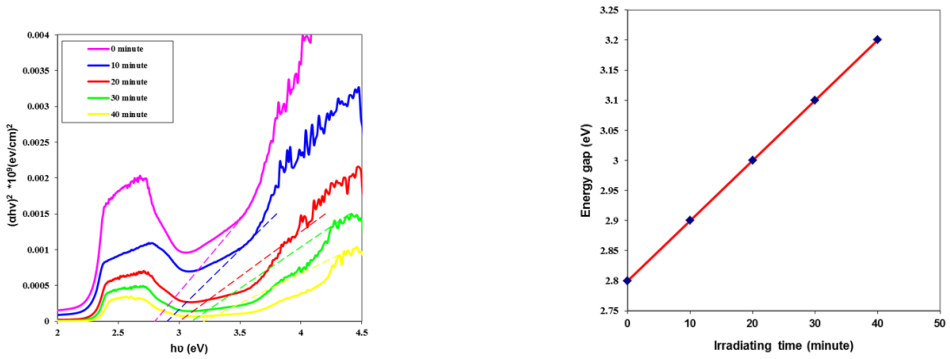

(**a**) (**b**)

Figure 11. PVA/MO energy gap and direct energy gap as a function of irradiation time: (**a**) Energy gap $(\alpha h\nu)^2$ for PVA/MO at different laser irradiation times (0, 10, 20, 30, and 40 min); (**b**) Direct energy gap as a function of irradiation time for PVA/MO at a 480 nm wavelength.

The optical constants for the PVA, MO, and PVA/MO composites, including the absorption coefficient, refractive index, extinction coefficient, and dielectric constants, are summarized in Tables 1–3.

Table 1. The optical constants of PVA thick films at 350 nm.

Time (min)	$\alpha \times 10^4$ (cm^{-1})	k	n	ε_{real}	ε_{imag} (s^{-1})	$\sigma_{op} \times 10^{14}$	E_g (eV)
0	0.107	0.0029	1.941	3.768	0.011	0.049	3.95
10	0.093	0.0025	1.840	3.388	0.009	0.041	4.01
20	0.082	0.0022	1.755	3.082	0.008	0.034	4.07
30	0.072	0.0020	1.672	2.796	0.006	0.028	4.09
40	0.061	0.0017	1.580	2.499	0.005	0.023	4.12

Table 2. The optical constants of MO thick films at 471 nm.

Time (min)	$\alpha \times 10^4$ (cm^{-1})	k	n	ε_{real}	ε_{imag} (s^{-1})	$\sigma_{op} \times 10^{14}$	E_g (eV)
0	0.087	0.0032	1.797	3.231	0.0118	0.0377	2.7
10	0.084	0.0031	1.773	3.145	0.0112	0.0359	2.9
20	0.080	0.0030	1.740	3.029	0.0105	0.0335	3.0
30	0.061	0.0023	1.583	2.507	0.0073	0.0233	3.1
40	0.056	0.0021	1.542	2.378	0.0065	0.0209	3.2

Table 3. The optical constants of PVA/MO composite thick films at 480 nm.

Time (min)	$\alpha \times 10^4$ (cm^{-1})	k	n	ε_{real}	ε_{imag} (s^{-1})	$\sigma_{op} \times 10^{14}$	E_g (eV)
0	0.054	0.0020	1.953	3.816	0.0081	0.0255	2.4
10	0.038	0.0014	1.718	2.951	0.0051	0.0159	2.5
20	0.031	0.0012	1.597	2.553	0.0038	0.0121	2.6
30	0.026	0.0010	1.515	2.295	0.0031	0.0097	2.7
40	0.023	0.0008	1.446	2.092	0.0025	0.0079	2.8

4. Conclusions

This investigation delineates the synthesis and characterization of thick films composed of polyvinyl alcohol (PVA), methyl orange (MO), and a PVA/MO composite, which were meticulously prepared by solubilizing measured quantities of PVA and MO powders in distilled water at a controlled temperature of 90 °C. The subsequent casting process

resulted in uniform films with reproducible thicknesses. This research focused on alterations in the optical properties of these films due to violet laser irradiation. A systematic decrease in the absorbance spectra with increasing irradiation times was observed across all samples, indicating photo-induced modifications in the material structure. Concurrently, the photonic energy gaps were found to widen with increased laser exposure, suggesting alterations in the electronic band structure conducive to photovoltaic applications. Furthermore, a comprehensive analysis revealed that critical optical parameters, including the absorption coefficient, extinction coefficient, refractive index, and dielectric constants, uniformly decreased as a function of the irradiation time. This trend is indicative of the laser-induced densification of the material's structure or a photochemical modification leading to a more ordered state, which has profound implications for enhancing the efficiency of optoelectronic devices. The outcomes of this study not only contribute to the fundamental understanding of polymer and dye interactions under laser irradiation but also pave the way for the development of novel materials with tailored optical properties. These materials have potential applications in a broad spectrum of fields, including photovoltaic systems, optical filters, and sensors, thereby holding promise for future technological advancements in material science.

Author Contributions: Methodology and writing—original draft preparation, A.H.A.-a.; validation, S.M.T.; formal analysis, N.A.A.; investigation, S.M.T.; resources, N.A.A.; data curation, S.M.T.; writing—review and editing, A.H.A.-a. All authors have read and agreed to the published version of the manuscript.

Funding: This research received no external funding.

Institutional Review Board Statement: Not applicable.

Informed Consent Statement: Not applicable.

Data Availability Statement: All the data used in the experiment have been made available in the present article.

Conflicts of Interest: The authors declare no conflicts of interest.

References

1. Ebewele, R.O. *Polymer Science and Technology*; CRC Press: New York, NY, USA, 1995; Volume 16, p. 3.
2. Nagarkar, R.; Patel, J. Polyvinyl Alcohol: A Comprehensive Study. *Acta Sci. Pharm. Sci.* **2019**, *3*, 34–44.
3. Patachia, A.P.; Valente, A.J.M. (Eds.) *Poly (vinyl alcohol) [PVA]-Based Polymer Membranes*; Nova Science Publishers: New York, NY, USA, 2009.
4. Jiang, S.; Liu, S.; Feng, W. PVA hydrogel properties for biomedical application. *J. Mech. Behav. Biomed. Mater.* **2011**, *4*, 1228–1233. [CrossRef]
5. Demerlis, C.C.; Schoneker, D.R. Review of the oral toxicity of polyvinyl alcohol (PVA). *Food Chem. Toxicol.* **2003**, *41*, 319–326. [CrossRef]
6. Giri, M.; Singh, D.; Lal, J.; Jaggi, N.; Singh, N.; Jaiswal, R.M.P. Absorption and Fluorescence Spectra of Methyl Orange in Aqueous Solutions. *Atti Fond. Giorgio Ronchi ANNO LXVII* **2012**, *2*, 255.
7. Al-kadhemy, M.F.H.; Saeed, A.A.; Kadhum, F.J.; Mazloum, S.A.; Aied, H.K. The effect of (He–Ne) laser irradiation on the optical properties of methyl orange doped PVA films. *J. Radiat. Res. Appl. Sci.* **2014**, *7*, 371–375. [CrossRef]
8. Bujdák, J. Controversial Issues Related to Dye Adsorption on Clay Minerals: A Critical Review. *Molecules* **2023**, *28*, 6951. [CrossRef]
9. Mohammadi, N.; Khani, H.; Gupta, V.K.; Amereh, E.; Agarwal, S. Adsorption process of methyl orange dye onto mesoporous carbon material-kinetic and thermodynamic studies. *J. Colloid Interface Sci.* **2011**, *362*, 457–462. [CrossRef]
10. Mohammed, H.S. Study the Effect of Immobilization on Electrostatic Potential for Methyl Orange Dye. *Muthanna J. Pure Sci.* **2018**, *5*, 38–43. [CrossRef]
11. Bhat, R.; Mohan, N.; Sharma, S.; Rao, S. Influence of Seawater Absorption on the Hardness of Glass Fiber/Polyester Composite. *J. Comput. Mech. Manag.* **2022**, *1*, 1–10. [CrossRef]
12. Singh, H.; Singh, K.; Vardhan, S. Enhancing Aluminum Matrix Composites with Hexagonal Boron Nitride (hBN) Particulates: A Comprehensive Review. *J. Comput. Mech. Manag.* **2023**, *2*, 5. [CrossRef]
13. Srikanth, V.; Kowshik, S.; Narasimha, D.; Patil, S.; Samanth, K.; Rathee, U. Finite Element Modelling and Analysis of Fiber Reinforced Concrete under Tensile and Flexural Loading. *J. Comput. Mech. Manag.* **2022**, *1*, 11–17. [CrossRef]
14. Chawla, K.K. *Composite Materials*; Springer: New York, NY, USA, 2012. [CrossRef]
15. Naik, N.; Suresh, P.; Yadav, S.; Nisha, M.P.; Arias-Gonzáles, J.L.; Cotrina-Aliaga, J.C.; Bhat, R.; Jalageri, M.D.; Kaushik, Y.; Kunjibettu, A.B. A Review on Composite Materials for Energy Harvesting in Electric Vehicles. *Energies* **2023**, *16*, 3348. [CrossRef]

16. Hiremath, P.; Viswamurthy, S.R.; Shettar, M.; Naik, N.; Kowshik, S. Damage Tolerance of a Stiffened Composite Panel with an Access Cutout under Fatigue Loading and Validation Using FEM Analysis and Digital Image Correlation. *Fibers* **2022**, *10*, 105. [CrossRef]
17. Mohan, N.; Sharma, S.; Bhat, R. A Comprehensive Study of Glass Fibre Reinforced Polymer (GFRP) Drilling. *Int. J. Mech. Prod. Eng. Res. Dev.* **2019**, *9*, 1–10.
18. Nowakowski, K.A. Laser Beam Interaction with Materials for Microscale Applications. Doctoral Dissertation, Worcester Polytechnic Institute, Worcester, MA, USA, 2005.
19. Hammood, A.; Al-Aarajiy, M. *Preparation and Characterization of NiPc/Si Organic Solar Cell*; University of Baghdad: Baghdad, Iraq, 2014.
20. Burns, G. *Solid State Physics*; Cambridge University Press: New York, NY, USA, 1985.
21. Hasan, M.; Khaleel, N. *Study the Linear and Nonlinear Optical Properties for Methylene Blue Dye Doped SiO_2 Nanoparticles*; University of Babylon: Babylon, Iraq, 2022.
22. Ejam, A. A.; Wahhab, N.A.A. Concentration effect on the optical properties of laser irradiation copper phthalocyanine (CuPc blue) solution. *NeuroQuantology* **2022**, *20*, 1–15. [CrossRef]
23. AbdulWahhab, N.A. Optical properties of SnO_2 thin films prepared by pulsed laser deposition technique. *J. Opt.* **2020**, *49*, 41–47. [CrossRef]
24. Nasir, E.M.; Hussein, M.T.; Al-Aarajiy, A.H. Investigation of Nickel Phthalocyanine Thin Films for Solar Cell Applications. *Adv. Mater. Phys. Chem.* **2019**, *9*, 158–173. [CrossRef]
25. Abdullah, O.G.; Saber, D.R. Optical absorption of Polyvinyl alcohol films doped with Nickel Chloride. *Appl. Mech. Mater.* **2012**, *110–116*, 177–182. [CrossRef]
26. Habubi, N. F.; Chiad, S.S. Optical Properties of Doped Polymers. *Diyala J. Pure Sci.* **2017**, *7*, 153–161.
27. Sólyom, J. *Fundamentals of the Physics of Solids, Volume 1 Structure and Dynamics*; Springer: New York, NY, USA, 2007.
28. Azim-Araghi, M.E.; Krier, A. Optical characterization of chloroaluminium phthalocyanine (ClAlPc) thin films. *Pure Appl. Opt. J. Eur. Opt. Soc.* **1997**, *6*, 443.. [CrossRef]
29. Thampraphaphon, B.; Phosri, C.; Pisutpaisal, N.; Thamvithayakorn, P.; Chotelersak, K.; Sarp, S.; Suwannasai, N. High Potential Decolourisation of Textile Dyes from Wastewater by Manganese Peroxidase Production of Newly Immobilised Trametes hirsuta PW17-41 and FTIR Analysis. *Microorganisms*. **2022**, *10*, 992. [CrossRef] [PubMed]
30. Mahendia, S.; Tomar, A. K.; Chahal, R. P.; Goyal, P.; Kumar, S. Optical and structural properties of poly(vinyl alcohol) films embedded with citrate-stabilized gold nanoparticles. *J. Phys. D Appl. Phys.* **2011**, *44*, 20. [CrossRef]